IMAGING OF REFLECTOR IN THE EARTH WITH WAVELET TRANSFORM①

Song, Shougen He, Jishen Rui, Jiagau
Department of Geolgogy, Central South University of Technolog, Changsha 410083

ABSTRACT

With wavelet transform, a new inverse and imaging method is proposed to the seismic inverse problem for two and one—half dimensional (2. 5D) velocity variations. Copmaring with the reflection function method presented by Bleistein *et al* (1985), proposed method has the advantages of that can be used to analyze and suppress the infection of the limited band width of observation in frequency.

Key words: inversion imaging wavelet

1 INTRODUCTION

This paper is motivated by the paper by Bleistein and others (1985, and 1979)[1, 2]. The reflection function method presented by them produces the pseudo-image about the reflector in the earth when the observed data are limited in frequence domain. So, it is necessary to find new inverse operator, which can analyze and suppress the effect of the limited band width of the observation in frequency.

First, we introduce a right-handed coordinate system $x=(x_1, x_2, x_3)$ with x_3 being positive in the downward direction into the earth. The observed field is the backscatter response from acoustic point source set off at every point $\zeta = (\zeta_1, \zeta_2, 0)$, on the surface of the earth. We assume that the total field $u(x, \zeta, \omega)$ is the solution of three dimensional Helmhotz equation, with point source at $\zeta = (\zeta_1, \zeta_2, 0)$:

$$\nabla^2 u(x, \zeta, \omega) + \frac{\omega^2}{v^2} u(x, \zeta, \omega) = -\delta(x_1 - \zeta_1)\delta(x_2 - \zeta_2)\delta(x_3) \quad (1)$$

with the sommerfeld radiation conditions:

$$\text{ru bounded, } r\left[\frac{\partial u}{\partial r} - \frac{i\omega}{v} u\right] \to 0, \text{ as } r \to \infty \quad (2)$$

where $r = |x|$, $v = v(x)$ is the wavespeed we seek.

The wavespeed is represented as a perturbation on a known reference speed, $c(x)$, expressed as

$$\frac{1}{v^2(x)} = \frac{1}{c^2(x)}[1 + \alpha(x)] \quad (3)$$

The total field $u(x, \zeta, \omega)$ is decomposed into an incident field $u_i(x, \zeta, \omega)$ and the scattered field $u_s(x, \zeta, \omega)$, that is

$$u(x, \zeta, \omega) = u_i(x, \zeta, \omega) + u_s(x, \zeta, \omega) \quad (4)$$

Similar to Eq. (25) in the paper by Bleistein *et al* (1985), we have, for 2. 5 D case

$$\alpha(x) = \frac{8c_0^3}{i\pi^2}\int dk_1 dk_3 d\zeta_1 dt \frac{k_3}{\omega^2} t u_s(\zeta, \zeta, t) \times e^{2ir^{-}k_1(x_1 \quad \zeta_1) + k_3 x_3 - i\omega t} \quad (5)$$

in which $\omega = c_0 \text{sgn}(k_3) \sqrt{k_1^2 + k_3^2}$

Because we have used the Born approximation and the high frequency assumption to get the formula (5), the $\alpha(x)$ in Eq. (5) is different with the true unknown $\alpha(x)$. Especially, when the subsurface velocity variation is not small and observed data is band-limited in frequency and contains noise, how much information of the true unknown $\alpha(x)$ that the $\alpha(x)$ in Eq. (5) contains is unclear.

In this paper, a new inversion method with

① Received Dec 17, 1993

two dimension wavelet transform is presented. The detection of the singularities of the $a(\boldsymbol{x})$ in Eq. (5) with multiscale wavelet transform is studied in section 2, and the relation between the interior surface with the modulus maxima of the wavelet transforms of the $a(\boldsymbol{x})$ in Eq. (5) is investigated.

Second, we study the infection of the limited band width of observation in frequency. But, how to suppress the noise, which is caused by the noise in observed data, from $a(\boldsymbol{x})$, we will study it in another paper.

2 THEORY

We choose two dimensional wavelet function $\psi^1(x)$ and $\psi^3(x)$ and as similar as Mallat and others (1992)[4]:

$$\psi^i(x) = \frac{\partial Q(x)}{\partial x}, \quad i = 1, 3, \quad x = (x_1, x_3) \tag{6}$$

in which $Q(x) = \frac{1}{2\pi} e^{-\frac{x_1^2 + x_3^2}{2}}$ is Gaussian function.

Let $Q_s(x) = \frac{1}{s^2} Q(\frac{x}{s})$ and

$$\psi^i_s(x) = \frac{1}{s^2} \psi^i(\frac{x}{s}) \tag{7}$$

$$W^i_s a(x) = (a * \psi^i_s)(x) = s \frac{\partial}{\partial x_i}(a * Q_s)(x) \tag{8}$$

where " * " is convolution operator, $i = 1, 3$.

The two dimensional wavelet transform of $a(\boldsymbol{x})$ is given by

$$W_s a(x) = \begin{pmatrix} W^1_s a(x) \\ W^3_s a(x) \end{pmatrix} = \begin{pmatrix} s \frac{\partial}{\partial x_1} a * Q_s(x) \\ s \frac{\partial}{\partial x_3} a * Q_s(x) \end{pmatrix} = s \nabla (a * Q_s)(x) \tag{9}$$

where "∇" is the two dimensional gradient operator.

With the help of setting $|W_s a(\boldsymbol{x})| = [|W^1_s a(\boldsymbol{x})|^2 + |W^3_s a(\boldsymbol{x})|^2]^{1/2}$, in the following we can prove that the value of $|W_s a(\boldsymbol{x})|$ is maximal when $\boldsymbol{x}$ is on the interior surface in the earth. So we know the position of subsurface by detecting the maxima of $|W_s a(\boldsymbol{x})|$.

2.1 *For the Single Tilted Plane Case*

As shown in Fig. 1, suppose the equation of tilted plane β is $x_1 \sin\theta + x_3 \cos\theta - h\cos\theta = 0$, with speed $v = c_0$ above the plane and speed $v = c_1$ below the plane. Let $\zeta = (\zeta_1, 0, 0)$ is a point on the line of observation. Suppose a unite impulse is set off at the surface, the reflected data at the surface can be approximated by

$$u_s(\zeta, t) = R \frac{\delta(t - 2l/c_0)}{8\pi l} \tag{10}$$

where $l = h\cos\theta - \zeta_1 \sin\theta$, $R = \frac{c_1 - c_0}{c_1 + c_0}$ is the normal incident reflection coefficient.

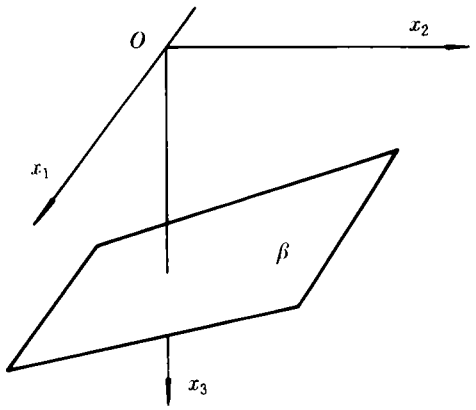

Fig. 1 Model for tilted plane

The data $u_s(\zeta, t)$ are substituted into Eq. (5) and the calculations are carried out, one obtains

$$a(x) = \frac{2R}{\pi} \int_{-\infty}^{\infty} \frac{d\omega}{i\omega} e^{2i\omega \cdots t_1 \sin\theta - (h - x_3)\cos\theta / c_0} \tag{11}$$

where $\omega = c_0 k_3 \sec\theta$

Substituting Eq. (11) into Eq. (8), one obtains

$$|W^1_s a(x)| = -\frac{2Rs\sin\theta}{\pi^2} \int_{-\infty}^{\infty} d\omega \times \int_{-\infty}^{\infty} e^{2i\omega (y_1 - x_1)\sin\theta - (h - y_3 - x_3)\cos\theta / c_0} \times \frac{1}{s^2} e^{-\frac{y_1^2 + y_3^2}{2s^2}} dy_1 dy_3 \tag{12}$$

and

$$W^3_s a(x) = -\frac{2Rs\cos\theta}{\pi^2} \int_{-\infty}^{\infty} d\omega \times \int_{-\infty}^{\infty} e^{2i\omega (y_1 - x_1)\sin\theta - (h - y_3 - x_3)\cos\theta / c_0} \times \frac{1}{s^2} e^{-\frac{y_1^2 + y_3^2}{2s^2}} dy_1 dy_3 \tag{13}$$

By the well known Fourier transform

$$\int_{-\infty}^{\infty} e^{i(\omega x - x^2/2)} dx = (2\pi)^{1/2} e^{(-\omega^2/2)} \tag{14}$$

one obtains

$$W_s^1a(x) = (-2R\sqrt{2}/\sqrt{\pi})\sin\theta \times e^{-\frac{1}{2s^2}[-x_1\sin\theta+(h-x_3)\cos\theta]^2} \quad (15)$$

$$W_s^3a(x) = -2R\sqrt{2}/\sqrt{\pi}\cos\theta \times e^{-\frac{1}{2s^2}[-x_1\sin\theta+(h-x_3)\cos\theta]^2} \quad (16)$$

Due to $|W_sa(x)| = \sqrt{|W_s^1a(x)|^2 + |W_s^3a(x)|^2}$, from Eqs. (15) and (16)

$$|W_sa(x)| = \frac{4Rc_o}{\sqrt{2\pi}}e^{-\frac{1}{2s^2}[-x_1\sin\theta+(h-x_3)\cos\theta]^2} \quad (17)$$

Eq. (17) implies that, when $-x_1\sin\theta + (h - x_3)\cos\theta = 0$, the value of $|W_sa(x)|$ is maximal. Noting that the equation of the tilted plane β is $x_1\sin\theta + x_3\cos\theta - h\cos\theta = 0$, So the maxima of $|W_sa(x)|$ correspond to the tilted plane β. Therefore, we know the position of subsurface in the earth by detecting the maxima of $|W_sa(x)|$.

Next, we investigate the infection of the limited band width of the observation in frequency. At this case, Eqs. (12) and (13) reduce to

$$W_s^1a(x) = -\frac{2Rs\sin\theta}{\pi^2}\int_{\omega_o}^{\omega_1} I(\omega)d\omega \quad (18)$$

$$W_s^3a(x) = -\frac{2Rs\cos\theta}{\pi^2}\int_{\omega_o}^{\omega_1} I(\omega)d\omega \quad (19)$$

here

$$I(\omega) = e^{-a\omega^2+ib} \quad (20)$$

$$a = \frac{2s^2}{c_o^2},$$

$$b = \frac{2[-x_1\sin\theta + (h - x_3)\cos\theta]}{c_o} \quad (21)$$

By Eq. (20), first we calculate the following integral:

$$Z_1(a, b) = \int_{\omega_0}^{\omega_1} e^{-a\omega^2}\cos b\omega d\omega,$$

$$Z_2(a, b) = \int_{\omega_0}^{\omega_1} e^{-a\omega^2}\sin b\omega d\omega$$

one obtains

$$Z_1(a, b) = e^{-\frac{b^2}{4a}}\{\int_{\omega_0}^{\omega_1} e^{-a\omega^2}d\omega + \int_o^b [e^{-a\omega_1^2}\sin\tau\omega_1 - e^{-a\omega_0^2}\sin\tau\omega_0]\frac{1}{2a}e^{\frac{\tau^2}{4a}}d\tau\} \quad (23)$$

$$Z_2(a, b) = e^{-\frac{b^2}{4a}}\int_o^b [e^{-a\omega_1^2}\cos\tau\omega_1 - e^{-a\omega_0^2}\cos\tau\omega_0]\frac{1}{2a}e^{\frac{\tau^2}{4a}}d\tau \quad (24)$$

By Eqs. (20), (23)and (24), from Eqs. (18) and (19), one obtains

$$W_s^1a(x) = -\frac{4Rs\sin\theta}{c_0\pi}[e^{-\frac{b^2}{4a}}\int_{\omega_0}^{\omega_1} e^{-a\omega^2}d\omega + e^{-\frac{b^2}{4a}}Z(a, b, \omega_0, \omega_1)] \quad (25)$$

$$W_s^3a(x) = -\frac{4Rs\cos\theta}{\pi^2}[e^{-\frac{b^2}{4a}}\int_{\omega_0}^{\omega_1} e^{-a\omega^2}d\omega + e^{-\frac{b^2}{4a}}Z(a, b, \omega_0, \omega_1)] \quad (26)$$

in which,

$$Z(a, b, \omega_0, \omega_1) = \int_o^b \frac{1}{2a}[e^{-a\omega_1^2}\sin\tau\omega_1 - e^{-a\omega_0^2}\sin\tau\omega_o]e^{\frac{\tau^2}{4a}}d\tau + i\int_o^b \frac{1}{2a}[e^{-a\omega_1^2}\cos\tau\omega_1 - e^{-a\omega_0^2}\cos\tau\omega_0]e^{\frac{\tau^2}{4a}}d\tau \quad (27)$$

From Eq. (27), we have the following inequality

$$|e^{-\frac{b^2}{4a}}Z(a, b, \omega_0, \omega_1)| \leqslant \frac{1}{a}(e^{-a\omega_1^2} + e^{-a\omega_0^2})e^{-\frac{1}{4a}(b^2-\tau_0^2)} \quad (28)$$

where $\tau_0 \in (0, b)$ or $\tau_o \in (b, 0)$.

From Eqs. (25) and (26), and inequality (28), we obtain

$$|W_sa(x)| = \frac{4Rs}{c_0\pi}e^{-\frac{b^2}{4a}}|\int_{\omega_0}^{\omega_1} e^{-a\omega^2}d\omega + Z(a, b, \omega_0, \omega_1)| \quad (29)$$

Especially, as $\omega_0 \to -\infty$ and $\omega_1 \to +\infty$, from Eq. (29), one obtains

$$|W_sa(x)| = 4RCo/\sqrt{2\pi}e^{-\frac{1}{2s^2}[-x_1\sin\theta+(h-x_3)\cos\theta]^2} \quad (30)$$

This equation is the same with Eq. (17). From Eq. (29) when the observed data is limited-band in frequency, we know that, as $b = 0$, that is, $x_1\sin\theta + (x_3 - h)\cos\theta = 0$, the value of $|W_sa(x)|$ is maximal.

Therefore, we still know the position of interior surface by detecting the modulus maxima of $W_sa(x)$, for the limited band case.

2.2 *At the General Case*

Suppose the equation of interior surface β is $f(x_1, x_3) = 0$, and for x "close enough" to the surface β, there will be only one perpendicular from x to β, as Fig. 2 shows.

In the following we can prove that the value of $|W_sa(x)|$ is maximal, when x is on the surface.

Similarity to Eq. (51) in the paper by Bleistein and others (1985)[1], we have

$$a(x) = \frac{8x_3\sqrt{c_o}}{\sqrt{\pi}\ i}\int\frac{d\zeta}{\rho^{3/2}}\int d\omega\frac{\sqrt{|\omega|}}{\omega}\frac{1}{i}$$

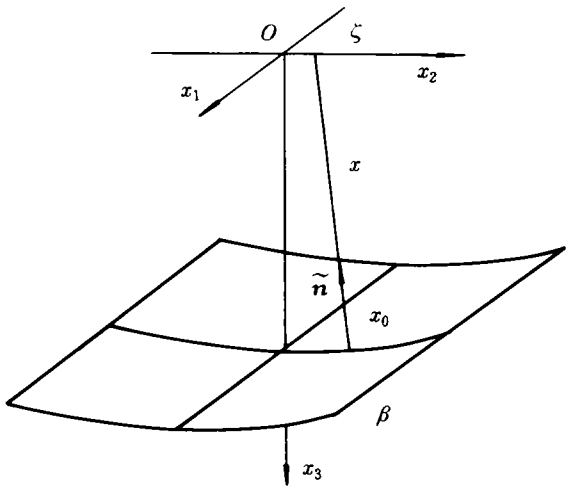

Fig. 2 Model for 2D curved surface

$$\times \left[\frac{\partial}{\partial\omega}u_s(\zeta,\ \omega)\right]e^{\left[-2i\omega\rho/c_o+i\,\mathrm{sng}(\omega)\frac{\pi}{4}\right]} \qquad (31)$$

Here,

$\rho = \sqrt{(x_1-\zeta_1)^2+x_3^2}$,

$\zeta = (\zeta_1,\ o,\ o)$, and

$$u_s(\zeta,\ \omega) = \int_0^\infty t u_s(\zeta,\ t)e^{i\omega t}dt. \qquad (32)$$

For $u_s(\zeta,\ \omega)$, we use the kirchoff approximation backscattered field, completely similar to Eq. (67) by Bleistein and others (1985)[1], we obtain

$$\alpha(x) = \frac{R_n}{\sqrt{|1-nk\sigma|}}\frac{1}{\pi}\int e^{2i\omega\sigma/c_o}\frac{1}{i\omega}d\omega \qquad (33)$$

where R_n, n, k and σ are the same with those in Eq. (67) by Bleistein and others (1985)[1].

Because, $r-\rho=\sigma$, with $\sigma>0$ when x is above β and $\sigma<0$ when x is below β, σ denotes the signed distance along the normal vector n. Given a point x close enough to surface β, drop perpendicular from x to β and x_o is the foot of the perpendicular. At the point x_o, the normal vector n is

$$n = (f'_{x_1}(x_0),\ 0,\ f'_{x_3}(x_0))$$

Hence , from above discussion, we know that there exists a factor $\mu>o$ so that

$$\sigma = \mu[f'_{x_1}(x_0)(x_0-x_{01}) + f'_{x_3}(x_0)(x_3-x_{03})] \qquad (34)$$

By Eqs. (33) and (34), one obtains

$$\alpha(x) = \frac{R_n}{\sqrt{|1-nk\sigma|}}\frac{1}{\pi} \times \int e^{2i\omega\mu[f'_{x_1}(x_0)(x_1-x_{01})+f'_{x_3}(x_0)(x_3-x_{03})]/c_0}\frac{1}{i\omega}dw \qquad (35)$$

where the domain of integration were $(-\infty,\ \infty)$ or (ω_0,ω_1)

Similar to Eq. (29), if x is near enough to surface β, one obtains

$$|W_s\alpha(x)| \approx \frac{4R_n s}{c_o\sqrt{|1-nk\sigma|}}e^{\left(-\frac{t_0^2}{4a}\right)} \left|\int_{\omega_0}^{\omega_1}\exp(-a\omega^2)d\omega + Z(a,\ b,\ \omega_0,\ \omega_1)\right| \qquad (36)$$

where

$$a = 2s^2/c_0^2[f'^2_{x_1}(x_0) + f'^2_{x_3}(x_0)],$$

$$b = 2[f'_{x_1}(x_0)(x_1-x_{01}) + f'_{x_3}(x_0)(x_3-x_{03})/c_0$$

$Z(a,\ b,\ \omega_0,\ \omega_1)$ satisfies the Eq. (27).

Eq. (36) implies that as $b=0$, i.e. $x_1=x_{01}$ and $x_3=x_{03}$, the value of $|W_s\alpha(x)|$ is maximal. This means that, when x is on the surface, the modulus value of $W_s\alpha(x)$ is maximal.

3 NUMERICAL EXPERIMENT AND DISCUSSION

Comparing with the reflection function method introduced by Bleistein (1985[1], and 1979[2]), based on Eqs. (29) and (36), we can not only detect more precisely the location of the reflector, but also analyse the effect of the limited band nature of the input data. Therefore, the method in this paper can eliminate the pseudo-image problem of the reflection function method.

In Fig. 1, take $\theta=15°$, $c_0=4500$ m/s. , $c_1=5500$ m/s and $h=2000$ m. For this model, the reflection function $\beta(x)$ in Refs. [1] and [2] is

$$\beta(x) = \frac{1}{10}\delta_B\{x_1\sin 15° + (2000 - x_3)\cos 15°\} \qquad (37)$$

where $\delta_B(\cdot)$ is a limited-band Delta function.

Fig. 3(a) is a 10～50 Hz band width representation of the reflection function $\beta(x)$ in Eq. (37). There exists obviously a pseudo-image about the titled plane in Fig. 3(a). But Fig. 3(b) is a 10～50 Hz bandwidth representation of $|W_s\alpha(x)|$ in Eq. (29), there is not any pseudo-image.

On the other hand, the wavelet operator $|W_s\alpha(x)|$ can suppress the noise in the observation. It will be studied in the continued paper.

(To page 8)

This is the optimum decision of blending which has considered the blending risk and its profits comprehensively, according to the present ore blending level.

6 INFLUENCE OF RANDOM ERROR ON ORE BLENDING

The influence of square deviation σ^2 of random error ε on expected blendig goal is sensitive. When different probabilities of real blending grade x, $y \in [53.5\%, 54.0\%]$, are given, then the corresponding optimum expected blending grades x^* and successful probabilities P are obtained as shown in Table 3.

Table 3 shows that the less the value σ^2, the less the value x^*, it means that more poor ore can be blended, meanwhile, the less the value σ^2, the more the successful possibility P of blending, the less the blending risk.

Hence, the mine must depend on technological improvements, improve management methods, and enhance control level of ore quality, then the mine can obtain not only a great deal of profits but also much more poor ore resources. On the other hand, when σ^2 decreases, the output grade fluctuation will reduce, it is beneficial for smelting material blending, and the follow-up benefit will be very considerable.

Table 3 Optimum expected blending grades x^* and successful probablities P

σ	x^*	$P(53.5 < x < 54.0)$
0.1	53.61	94.16
0.3	53.73	59.25
0.5	53.78	38.42
0.7	53.82	24.60

REFERRENCES

1 Qi, Guo-an *et al.* J of Mines, 1992, 1: 23—25.
2 Shu, Hang. J of Mine Tech, 1992, 3: 56—58.
3 Shu, Hang *et al.* J of Metal Mines, 1992, 3: 54—57.

(*From page 4*)

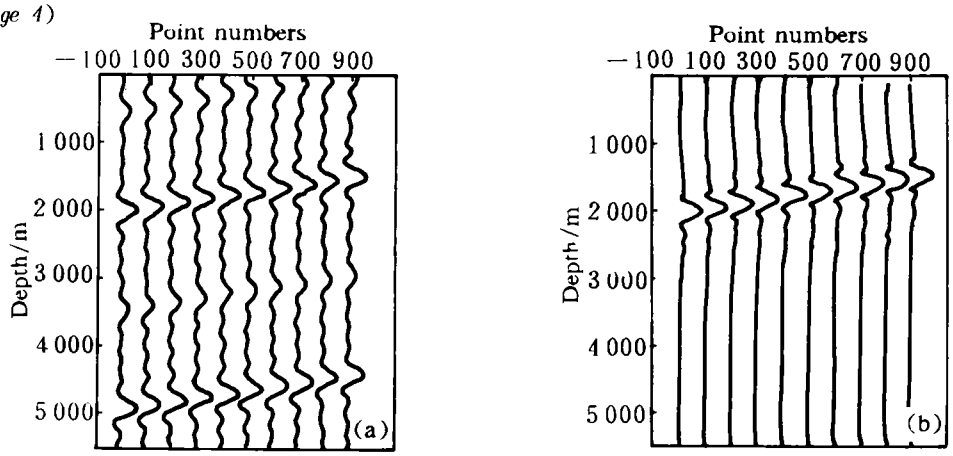

Fig. 3 A 10～50 Hz bandwidth representation of the reflection function $\beta(x)$ and the wavelet $|W_S\alpha(x)|$
(a)— $\beta(x)$; (b)— $|W_S\alpha(x)|$

REFERENCES

1 Bleistein, N, Cohen, J K; Hagin, F G. Geophysics, 1985, 50: 1253—1265.
2 Cohen, J K; Bleistein, N. Geophysics, 1979, 44: 1077—1087.
3 Grossman, A. In: Hazwinke M(ed), Wavelet transform and edge detection, in stochastic processes in physicsand Engineering, ed. M. Hazwinke, Dodrecht, Reidel. 1986.
4 Mallat, S; Hwang, W L. IEEE Trans On Information Theory. 1992, 38: 617—643.